Oxidation of Zigzag Carbon Nanotubes by Singlet O_2: Dependence on the Tube Diameter and the Electronic Structure

Yong-fan Zhang[†] and Zhi-feng Liu*

Department of Chemistry andCentre for Scientific Modeling and Computation, Chinese University of Hong Kong, Shatin, Hong Kong, P.R. China

Received: March 1, 2004; In Final Form: May 14, 2004

The chemisorption of singlet O_2 on the side wall of a series of zigzag (n,0) Single Walled Carbon Nanotubes (SWNTs) ($n = 6 \sim 15$) have been investigated by planewave/pseudopotential- based density functional theory. The process involves two steps, cycloaddition, followed by the breaking of an O−O bond with the formation of epoxy structures. The most stable adsorbate configurations have been determined for both steps. The results indicate that the saturation of a zigzag C−C bond induces less stress on a carbon nanotube than the saturation of an axial C−C bond. The formation of the epoxy structure is exothermic and the degradation of carbon nanotubes upon air exposure is possible for tubes with a diameter below 1 *nm*. Overall, the adsorption energy decreases with increasing tube diameter, and the electronic structure also affects the reactivity. Furthermore, the changes in electronic structures introduced by the adsorption of oxygen have also been examined.

Introduction

Since their discovery by Iijima in 1991,[1] carbon nanotubes have attracted a lot of attention, due to their remarkable physical properties and potential applications in nanoscale devices. Recently, exploring the changes of carbon nanotube properties through various modifications has become a topic of growing interest. It is well known that the properties of carbon nanotubes, such as transport and optical characteristics, are very sensitive to chemical modifications and sidewall functionalization.[2] Therefore, chemical processing of carbon nanotubes is critically important for the realization of the promises of this material. A single-walled carbon nanotube (SWNT) is formed by rolling a graphene sheet into a seamless cylinder. As a result, the curvature-induced misalignment of the π orbitals on the carbon atoms induces a local strain, and SWNTs are expected to be more reactive than a flat graphene sheet.[3,4] Just as in the case of fullerene chemistry,[5] the reactivity of SWNTs depends strongly on the curvature of the carbon framework, which is indicated by the carbon pyramidalization. It varies inversely with the tube diameters, and the smaller the diameter, the larger the pyramidalization angle and the more reactive for the corresponding SWNT. For example, it is difficult for HiPco (high-pressure decomposition of CO) tubes with small diameters to survive the treatment of oxidizing agents (such as HNO_3 or H_2SO_4). In contrast, the destruction of large diameter nanotubes produced by electric arc process requires more strongly oxidative conditions.[6,7] Electronic structure could also affect the chemical reactivity. Very recently, Strano et al.[8] reported that in the reactions of SWNTs with diazonium reagent, only the metallic and semimetallic tubes were reactive, while the semiconducting tubes were nearly excluded. Such differentiation in reactivity shows the potential for the selective functionalization of carbon nanotubes and for the separation and purification of mixed raw tubes.

O_2 is an important oxidative reagent, as it is present in air, and the reactions between O_2 and carbon nanotubes have important implications for the stability of carbon nanotubes upon air exposure. Increases in the oxidation rate for the carbon nanotubes have been reported upon UV illumination.[9] Experiments have shown that the electronic, transport, and magnetic properties of tubes are sensitive to air exposure,[10−13] and a semiconducting SWNT can be reversibly converted to a conductor by a small dose of adsorbed oxygen.[10] More recent measurements have shown that the main effect of oxygen physisorption is not to dope the bulk of the tube, but to change the barriers of the metal-semiconductor contact.[14,15]

A number of theoretical calculations have also been reported on the interaction between O_2 and carbon nanotubes. According to Density Functional Theory (DFT) calculations, the ground-state triplet O_2 can only physisorb on the tube walls, effecting the spin lattice relaxation rate.[12] The edge of a carbon nanotube is more reactive, and a number of precursor states could be formed.[16,17] For the more reactive singlet O_2, its adsorption on the tube wall was initially found to be unfavorable, with a reaction barrier around 1.5 eV for an (8,0) tube based on an extensive computational study using DFT method with a planewave basis set and pseudopotentials.[18] Similar conclusions were also reached in recent two-layer ONIOM calculations,[19] in which only the O_2 molecule and a fragment of the carbon nanotube, in the form of a bent ethylene or benzene, were treated at high accuracy level by the second-order Møller−Plesset perturbation theory, while the rest of the tube was treated by the universal force field method.

However, we have recently shown that spin-contamination is a serious problem in Sorescu et al.,[18] and the actual barrier is considerably lower at around 0.6 eV for an (8,0) tube and 0.9 eV for a (6,6) tube, leading to a cycloaddition product, which could be further transformed into a structure with the O−O bond broken and the two oxygen atoms each occupying an epoxy position, bridging two adjacent carbon atoms.[20] The overall process was found to be exothermic for the (8,0) tube. Similar findings were also reported by Froudakis et al.[21] for (4,4) or (5,5) tubes. These results raise the prospect for the degradation of carbon nanotubes exposed to air and sun light, which

* Corresponding author. E-mail: zfliu@cuhk.edu.hk.
[†] Permanent address: Department of Chemistry, Fuzhou University, Fuzhou, Fujian, 350002, P. R. China.

10.1021/jp049088j CCC: $27.50
Published on Web 07/01/2004

produces singlet O_2, similar to the degradation of natural rubber and synthetic plastics.

It is expected that for larger tubes, such an oxidation process would be less favorable because the reactivity of a carbon nanotube decreases with increasing tube diameter, as indicated in the calculated adsorption energy for the (6,6), (8,8) and (10,10) armchair tubes.[20] The exact nature of such a change is an open question and the subject of our investigation. In the present paper, we present a detailed, first-principles analysis of the singlet O_2 adsorption on a series of zigzag (n,0) SWNTs ($n = 6 \sim 15$). This series not only provides a systematic variation in the tube diameter, but also changes in the electronic structure. For a zigzag SWNT with the (n,0) index, it is semimetallic or metallic for $n = 3m$ (with m being an integer), and semiconducting otherwise.[22] As the SWNTs used in experiments are usually considerably larger than the (8,0) tube studied before, our work shall provide a more realistic evaluation on the potential degradation of carbon nanotubes upon air exposure.

Computational Method

The first principles total energy and electronic structure calculations were carried out within the framework of DFT with a plane wave basis set and pseudopotentials for the atomic cores,[23,24] as implemented in the Vienna ab initio simulation package (VASP).[25] The PW91 gradient correction was added to the local density exchange-correlation functional[26] and Vanderbilt ultrasoft pseudopotentials[27] were employed, with an energy cutoff of 396 eV for the plane-wave expansion. A nanotube was modeled by a periodically repeating supercell. With a tube lying along the c direction, the lattice parameters a and b were chosen to ensure a minimum distance of more than 9 Å between two nearest neighbors, so that the interactions between a tube and its periodic images were negligible. To avoid the adsorbate−adsorbate interaction, the value of c was set to double the length of the translation vector of the tube along the axial direction, which was determined first by minimizing the total energy. For the zigzag (n,0) SWNTs, the optimized lengths of c were around 8.5 Å. The Brillouin zones of the supercells were sampled only along the tube axis and the Monkhorst-Pack special k-point scheme was used,[28] producing two irreducible k points. The structural optimizations were performed until the final Hellmann−Feynman forces were smaller than 0.02 eV/Å. A similar setup has been used in the previous study of singlet O_2 interaction with (8,0) tube.[20] The optimized O−O bond length for both triplet and singlet O_2 were just below 1.24 Å, compared to the experimental values of 1.21 Å for triplet and 1.22 Å for singlet oxygen.[29] The calculated energy to excite an O_2 molecule from the $^3\Sigma_g^-$ state to the $^1\Delta_g$ state was about 1.08 eV, in reasonable agreement with the experimental result of 0.98 eV.[29]

The adsorption energy (E_{ads}) is defined by the expression

$$E_{ads} = E[\mathrm{SWNT} + \mathrm{O_2}] - (E[\mathrm{SWNT}] + E[\mathrm{O_2}]) \quad (1)$$

in terms of the total energy of an optimized pristine tube-(E[SWNT]), the singlet O_2 molecule(E[O_2]), and the tube-adsorbate system(E[SWNT + O_2]), all calculated using the same unit cell and k-points. A negative E_{ads} corresponds to an exothermic adsorption process. In addition, to describe the distortion of the SWNTs upon chemisorption, the deformation energy is determined by using the expression

$$E_{def} = E[\mathrm{Def} - \mathrm{SWNT}] - E[\mathrm{SWNT}] \quad (2)$$

where, the E[Def − SWNT] is the total energy of a deformed tube, calculated by considering only the contribution of the tube part in a SWNT−O_2 system.

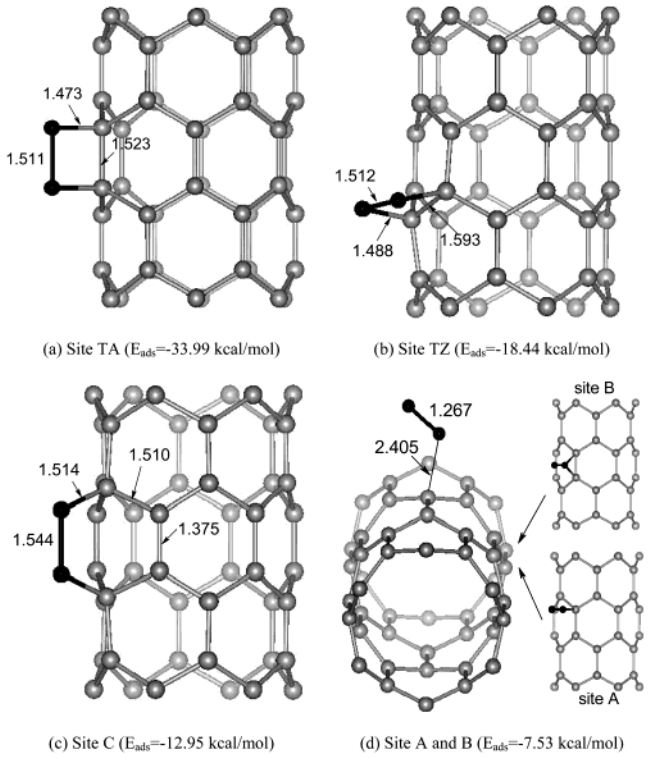

Figure 1. Possible cycloaddition structures on a (6,0) carbon nanotube, with the bond distance in Å. The adsorption energy is shown in parentheses. While sites TA, TZ, and C lead to stable chemisorption structures, sites A and B are unstable and are transformed into a physisorbed structure upon optimization.

To evaluate the atomic contribution to the electronic structure, we also performed DFT calculations on the band structures and density of states (DOS) with atomic basis functions, using the CRYSTAL program.[30] In these calculations, the standard 6-21G and 6-21G* basis sets were employed for C and O atoms, respectively, in the geometrical configurations optimized by plane wave calculations.

Results and Discussion

1. The Cycloaddition of Singlet O_2. A number of initial configurations for the singlet O_2 adsorption have been considered in our investigation, as shown in Figure 1. With O_2 being parallel to the tube surface, there are three possible configurations, including site TA, on top of an axial C−C bond; site TZ, on top of a zigzag C−C bond; and site C, above the center of a hexagonal carbon ring. It is also possible for the O_2 to be perpendicular to the tube surface, as in site B, with O_2 on top of an axial C−C bond in a bridge position, and site A, with O_2 on top of a C atom. However, sites A and B do not lead to stable structures and geometry optimizations produce only a physisorbed configuration with a tilted O_2 molecule (Figure 1d). On the other hand, the two sites, TA and TZ, lead to chemisorbed structures via cycloaddition, as shown in Figure 1, which has been previously reported,[18,20] and shall be the focus of our study.

Listed in Table 1 are the structural parameters and adsorption energy for the chemisorbed TA and TZ configurations, for all the (n,0) tubes studied with $n = 6$ to 15. For the (8,0) tube, our results are in good agreement with previous reports.[18,20] For the (9,0) and (10,0) tubes, significant differences are found for the calculated E_{ads}, compared with the recent investigation by

TABLE 1: The Calculated Adsorption Energy (E_{ads}) and Optimized Structural Parameters for the Cyclo-addition of Singlet O_2 on Zigzag (n,0) SWNTs, with $n = 6-15$, for Sites TA and TZ as Shown in Figure 1

	site TA[a]						site TZ[a]				
SWN T	diameter (Å)	C−C (Å)	C−O (Å)	O−O (Å)	E_{ads} (kcal/mol)	E_{def} (kcal/mol)	C−C (Å)	C−O (Å)	O−O (Å)	E_{ads} (kcal/mol)	E_{def} (kcal/mol)
(6,0)	4.80	1.523	1.473	1.511	−33.99	25.31	1.593	1.488	1.512	−18.44	21.98
(7,0)	5.58	1.530	1.479	1.509	−19.83	31.56	1.605	1.484	1.516	−12.21	24.93
(8,0)	6.35	1.527	1.481	1.510	−17.75	32.48	1.596	1.486	1.515	−9.02	26.24
(9,0)	7.13	1.529	1.487	1.508	−14.51	32.05	1.583	1.492	1.513	−5.36	27.22
(10,0)	7.90	1.532	1.491	1.507	−4.07	33.98	1.584	1.488	1.515	−0.35	27.51
(11,0)	8.71	1.531	1.490	1.508	−2.15	33.94	1.582	1.489	1.514	3.37	28.18
(12,0)	9.49	1.530	1.492	1.506	−2.83	33.92	1.571	1.495	1.512	3.09	28.92
(13,0)	10.24	1.533	1.497	1.506	3.03	34.84	1.575	1.492	1.514	5.82	29.23
(14,0)	11.01	1.530	1.494	1.508	2.77	34.60	1.572	1.493	1.514	8.18	29.99
(15,0)	11.77	1.533	1.498	1.506	0.71	33.70	1.568	1.495	1.511	5.61	29.66

[a] The distances listed are for those bonds on the cycloaddition adsorption sites.

Ricca and co-workers[19,31] using the ONIOM method, while similarity was found only in the geometrical configurations. The TA sites of the (9,0) and (10,0) tubes were previously found to be energetically favorable by −18.08 and −17.50 kcal/mol respectively, relative to the bare tube and a triplet O_2. In contrast, our results produce an endothermic energy of 10.38 and 20.82 kcal/mol with respect to the nanotube and triplet O_2. Only in respect to the singlet O_2, is an exothermic energy obtained, with −14.51 kcal/mol for a (9,0) tube and −4.07 kcal/mol for a (10,0) tube. This large discrepancy in E_{ads} is probably due to the model used in the ONIOM calculation, in which the system was divided into an inner layer treated at high accuracy level (MP2) and an outer layer treated by molecular mechanics. The inner layer was essentially composed of an O_2 and an ethylene molecule containing only one C−C bond.[19,31] Our recent study on the adsorption of ozone on a (5,5) carbon nanotube showed that in ONIOM calculations the adsorption energy was dependent on the size of the inner layer, and to obtain the correct results, a circumcoronene molecule with 54 C atoms was required to model a (5,5) tube.[32]

There is clearly a general trend that the value of $-E_{ads}$ for both the TA and TZ sites decreases as the diameter of the (n,0) zigzag tube increases (Figure 2a), similar to the trend observed for the (n,n) armchair tube.[20] For the TA site, the adsorption energy switches sign around $n = 12$, when the tube diameter is around 9.5 Å. For tubes with n larger than 12, the cycloaddition process becomes energetically unfavorable. A similar switching point is observed around $n = 10$ for the TZ site. This trend can be readily understood by the decrease of curvature on the tube surface and correspondingly a decrease in chemical reactivity, as the diameter increases.[3,33−35]

However, the curve of the adsorption energy versus the tube diameter is not smooth, as shown in Figure 2a, in contrast to the recently reported 1,3-dipolar cycloadditions on the armchair (n,n) tubes.[34] For instance, although the diameter for the (15,0) tube is larger than that for either the (13,0) or the (14,0) tube, the O_2 adsorption energy for (15,0) is less endothermic than that for the latter two. Similar deviation from the trend is also observed for the (9,0) and (12,0) tubes, and less dramatically for the TZ sites. Therefore, our results indicate that the smooth diameter dependence for the reactivity of the armchair (n,n) tubes observed in previous works cannot be directly applied to the case of the zigzag tubes.[34,35] This difference indicates that the electronic structure could also be a factor affecting the chemical reactivity of a tube, as observed in a recent experiment.[8] For the armchair (n,n) tubes, the band structure is always metallic, and the reactivity is mainly determined by the tube diameter. In contrast, the zigzag (n,0) tubes can either be metallic (for $n = 3m$) or semiconducting (for $n = 3m + 1$ and $3m + 2$). Our results indicate that the metallic tubes are more favorable for O_2 cycloaddition, which could be due to the higher density of states near the Fermi level that makes them more favorable for binding with the O_2 molecules. Within the general trend of decreasing reactivity with increasing diameter, the change in electronic structure produces fluctuations in the adsorption energy.

For site TA, the optimized lengths of C−C bond in the cycloaddition four-member ring are around 1.53 Å (Table 1), in comparison to the bond distance of a typical C−C σ bond around 1.54 Å and to the typical C−C distance around 1.42 Å on the bare tube. The elongation of the C−C bonds on the adsorption site indicates that the π bonding interaction between these two carbon atoms is saturated after the adsorption of O_2. As a result, the pristine tube is now distorted. The variation of the calculated deformation energies as defined in (2) for site TA is presented in Figure 2b, which singles out the contribution of tube deformation to the overall adsorption energy. On the whole, the value of E_{def} increases with increasing diameter of SWNT, which also makes it unfavorable for the cycloaddition on large tubes. However, the difference in the deformation energy, as n goes from 6 to 15, is within 10 kcal/mol, while the absolute value of adsorption energy decreases by around 30 kcal/mol, a large part of which should thus be attributed to the more favorable bonding geometry in the cycloaddition product for the small tubes.

The calculated cycloaddition structures on site TZ, also listed in Table 1, are similar to the TA structures, except that the lengths of the C−C bonds in the four-member ring are longer. This difference is due to the fact that the saturated C−C bond on site TZ is along the zigzag direction and is more strained than that in the axial direction. However, when the tube diameter increases, this difference is reduced, and accordingly, the difference in the C−C distance is reduced, as shown in Table 1. Compared with the TA site, the addition of singlet O_2 to the circumference C−C bond in the TZ site induces smaller distortion on the tube structure, and the value of E_{def} for site TZ is smaller than that for the TA structure for tubes with the same index. It indicates that the distortion along the radial direction is easier than that along the axial direction, which is in agreement with previous experiments on the deformation of carbon nanotubes.[36−38]

2. The Formation of Epoxide Structure. As identified in our previous work,[20] the chemisorbed O_2 can go through a further step of reaction to produce two O atoms, each occupying a bridge position between two carbon atoms. Similar epoxide structures have also been observed in the studies on the adsorption of oxygen atoms on SWNTs.[18,21,39−41] Here, we only consider the epoxy products derived from two favorable

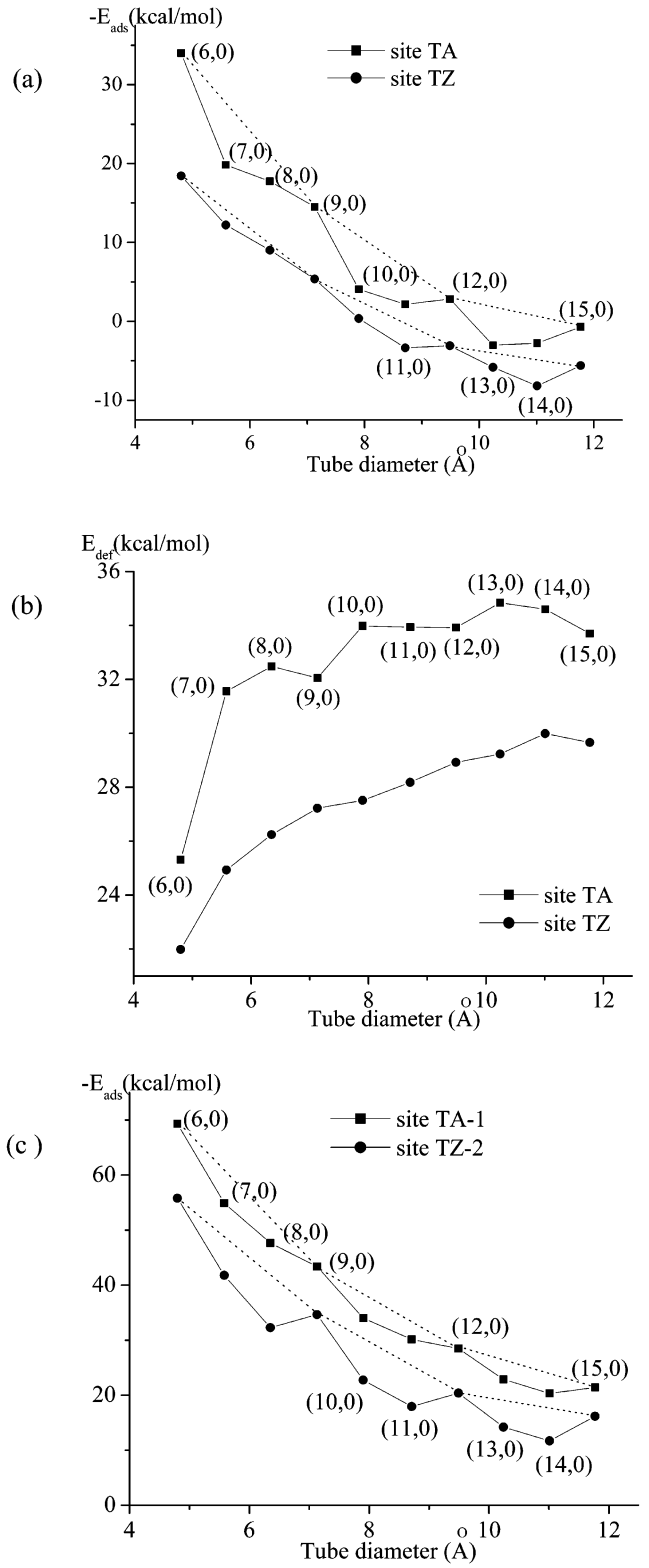

Figure 2. (a) Adsorption energy (E_{ads}) for the cycloaddition products; (b) Deformation energy (E_{def}) for the cycloaddition; (c) Adsorption energy (E_{ads}) for epoxy-like structures; all as a function of the tube diameter.

cycloaddition models, sites TA and TZ. For each site, there are two possible epoxide configurations, depending on whether the dissociated O atoms are in the same hexagonal carbon ring or not, as shown in Figure 3 for a (6,0) tube. The most favorable configurations are sites TA-1 and TZ-2, respectively, which will be the focus of our study.

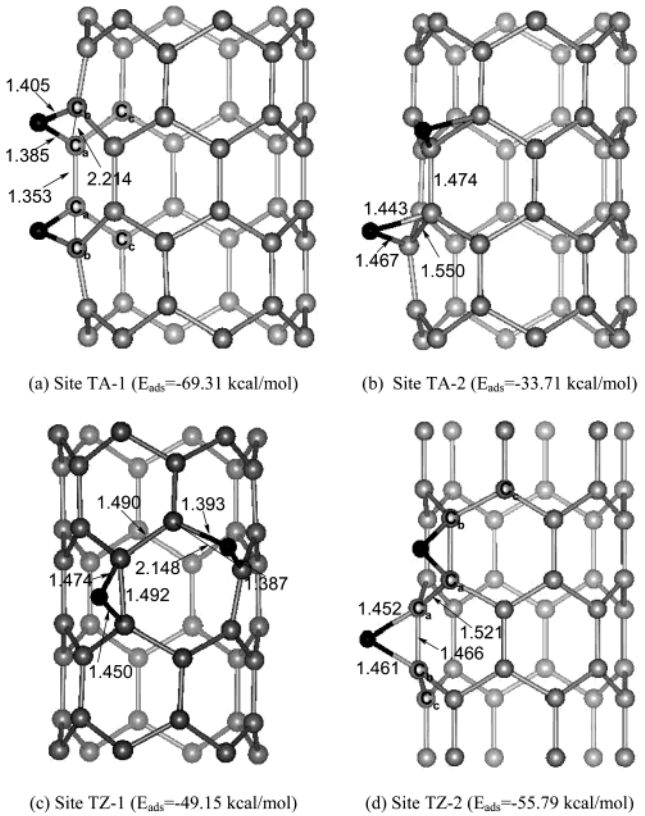

Figure 3. Epoxy-like structures for a (6,0) carbon nanotube, with the bond distances in Å. They are derived from the TA and TZ structures shown in Figure 1. In TA-1 and TZ-1, the two O atoms are in the same hexagonal ring, while in TA-2 and TZ-2 the two O atoms are in two neighboring hexagonal rings. Based on the adsorption energy, the TA-1 and TZ-2 structures are the most stable.

The parameters of the epoxy structures for all zigzag tubes are listed in Table 2. For the (n,0) tubes studied in this work, the C_a-C_b bond (labeled in Figure 3) in site TA-1 is actually broken, with the bond distance elongated to around 2.2 Å, in agreement with previous results.[39] At the same time, the C_a-C_a bond distance is decreased to ~1.36 Å, which is closer to the typical C−C double bond distance of ~1.34 Å and shorter than the typical C−C distance of ~1.42 Å for a bare tube. It indicates a strengthening of the C_a-C_a bond, as the C_a-C_b bond is broken. The C_a-C_c bond around 1.40 Å is only slightly reduced. For the TZ-2 structures, no C−C bond is completely broken. The C−C distances around the adsorption site are increased, compared to the bare tube. The largest increase is observed for the C_a-C_a bond, rather than the C_a-C_b bond in the case of the TA-1 site. As n increases, the differences among the three distances, C_a-C_b, C_a-C_a, and C_a-C_c, decrease. With $n > 8$, one additional structure is identified, which is similar to a TA-1 structure, except that the bridged C_a-C_b bond is not broken. Geometry parameters and adsorption energies for these structures are also listed in Table 2, and in terms of the adsorption energy, they are less favorable than either the corresponding TA-1 or the TZ-2 structures. For all three structures, the longest C−C bond (C_a-C_b in TA-1, and C_a-C_a in TZ-2) is along the zigzag direction, which is probably again due to the fact that it is easier to deform a carbon nanotube along the circumference direction than along the axial direction.[36−38]

The formation of epoxy structures is exothermic for both sites TA-1 and TZ-2 with respect to a bare tube and a singlet O_2 (Table 2), for all the zigzag tubes studied, and site TA-1 is more

TABLE 2: The Calculated Adsorption Energy (E_{ads}) and the Optimized Structure Parameters for the TA-1 and TZ-2 Epoxide-like Structures in the Second Step of O_2 Chemisorption on Zigzag (n,0) SWNTs with $n = 6-15$

	site TA-1[a]						site TZ-2[a]					
SW NT	C_a-C_b (Å)	C_a-C_a (Å)	C_a-C_c (Å)	C_a-O(Å)	E_{ads} (kcal/mol)	E_{def} (kcal/mol)	C_a-C_b (Å)	C_a-C_a (Å)	C_a-C_c (Å)	C−O (Å)	E_{ads} (kcal/mol)	E_{def} (kcal/mol)
(6,0)	2.214	1.353	1.412	1.395	−69.31	122.76	1.466	1.521	1.497	1.455	−55.79	21.12
(7,0)	2.195	1.366	1.401	1.396	−54.89	134.88	1.473	1.521	1.491	1.459	−41.76	28.28
(8,0)	2.205	1.360	1.404	1.395	−47.64	143.39	1.470	1.513	1.487	1.462	−32.27	27.97
(9,0)	2.217	1.362	1.398	1.392	−43.36	148.07	1.471	1.512	1.485	1.465	−34.63	25.89
	(1.572)[b]	(1.484)	(1.463)	(1.442)	(−23.44)							
(10,0)	2.196	1.369	1.397	1.392	−34.01	155.03	1.475	1.509	1.480	1.463	−22.73	29.03
	(1.586)	(1.482)	(1.458)	(1.439)	(−17.62)							
(11,0)	2.205	1.364	1.399	1.390	−30.11	158.04	1.474	1.507	1.479	1.466	−17.93	28.33
	(1.577)	(1.483)	(1.461)	(1.440)	(−13.42)							
(12,0)	2.216	1.365	1.396	1.388	−28.47	160.98	1.474	1.505	1.475	1.467	−20.36	28.16
	(1.551)	(1.488)	(1.467)	(1.447)	(−13.87)							
(13,0)	2.193	1.370	1.395	1.391	−22.87	163.22	1.476	1.505	1.473	1.467	−14.19	28.42
	(1.559)	(1.488)	(1.463)	(1.444)	(−10.45)							
(14,0)	2.202	1.366	1.396	1.387	−20.30	165.57	1.475	1.504	1.473	1.468	−11.69	28.70
	(1.558)	(1.487)	(1.463)	(1.445)	(−8.15)							
(15,0)	2.215	1.367	1.393	1.386	−21.40	166.32	1.477	1.505	1.474	1.469	−16.15	27.83
	(1.540)	(1.492)	(1.468)	(1.450)	(−10.92)							

[a] The labeling of atoms is shown in Figure 3. [b] The values of configurations where the bridge C_a-C_b bond is not broken are listed in parentheses.

stable than site TZ-2. They are also considerably more stable than the corresponding cycloaddition configurations (Table 1). Again, there is a trend of decreases for the value of $-E_{ads}$ as the tube diameter increases, as shown in Figure 2c, although even for a (15,0) tube, the largest tube studied, the adsorption energy remains exothermic. Similar to the cycloaddition step, the variation of E_{ads} for both sites TA-1 and TZ-2 is not a smooth function of the tube diameter, as adsorptions on metallic tubes are more favorable (Figure 2c).

For site TZ-2, the deformation energy changes only slightly from that for its corresponding cycloaddition structure (Tables 1 and 2). It indicates that the breaking of the O−O bond and the formation of the bridge structure do not add further strain to the tube, and the stabilization gained in the formation of epoxy structure is thus largely due to more favorable bonding interactions between the oxygen and carbon atoms. However, for the TA-1 structure, the deformation energy is more than quadrupled compared to the cycloaddition process. Obviously, it can be attributed to the breaking of the C_a-C_b bonds. The overall larger adsorption energy of TA-1 structure shows that the deformation energy must be well compensated by the more favorable C−O bonding, as indicated by a shorter C−O distance.

3. The Electronic Structures. Cycloaddition and epoxy formation both induce changes in the electronic structure, with the introduction of oxygen atoms and their orbitals. To understand these changes, we did additional calculations using the CRYSTAL program, which employed atomic basis functions and was better suited to the analysis of orbital characters.[30] These are also DFT calculations, with the PW91 exchange-correlation functionals, and the structures used are those optimized by the planewave/pseudopotential based DFT method as discussed in previous sections. The band structures calculated by these two methods are in good agreement with each other. Shown in Figure 4 are the band structures for the (9,0) and (10,0) tubes calculated by CRYSTAL, with the bands derived from significant contributions from oxygen orbitals marked by filled circles. For the cycloaddition models, sites TA and TZ, the bands originated from oxygen are mainly located in the regions around −0.5 eV and −3.5 eV for the occupied states, and around 3.0 eV for the unoccupied states, with the energies relative to the Fermi level. Based on the characters of the corresponding crystal orbitals, the unoccupied states near 3.0 eV are mainly due to the σ^* interactions between the O 2p orbitals. Below the Fermi level, the states near −0.5 eV are mainly due to the π^* interactions between O atoms, while the bonding interaction between O atoms contribute to the band around −3.5 eV. For the TA-1 and TZ-2 epoxy structure, the two oxygen atoms are well separated without any bonding interactions, and the band structure contains contributions from O atomic orbitals, which are located in the region $-3.0 \sim -1.0$ eV.

TABLE 3: The Band Gaps (eV) for the Pristine and Oxygen Adsorbed Tubes

	band gap (eV)				
SWNT Index	bare tube	site TA	site TZ	site TA-1	site TZ-2
(6,0)	0.0	0.0	0.0	0.0	0.0
(7,0)	0.382	0.217	0.428	0.267	0.314
(8,0)	0.757	0.372	0.673	0.662	0.237
(9,0)	0.162	0.193	0.116	0.165	0.419
(10,0)	0.804	0.194	0.696	0.411	0.483
(11,0)	0.929	0.467	0.492	0.707	0.246
(12,0)	0.108	0.113	0.040	0.167	0.275
(13,0)	0.679	0.173	0.579	0.351	0.385
(14,0)	0.712	0.414	0.376	0.572	0.228
(15,0)	0.030	0.016	0.044	0.164	0.196

As reported previously, the properties of SWNTs are sensitive to chemical modification, and in the case of the fluorinated SWNT, the tube can be insulating, semiconducting, or metallic, depending on the fluorination patterns.[42,43] The calculated band gaps for the pristine tubes, and the cycloaddition and epoxy products, are presented in Table 3. As is well-known, the band gap for zigzag SWNTs can be divided into three groups.[44] The tubes with $n = 3m$ have zero or very small gaps, those with $n = 3m + 1$ have nonzero gaps, and those with $n = 3m + 2$ have the largest band gaps. Such a pattern is well reproduced in our calculations, while changes in the band gap upon O_2 adsorption are observed.[45] Generally, for the semiconducing tubes ($3m + 1$ and $3m + 2$), the band gap is reduced for both the cycloaddition and epoxide structures. In the case of the (10,0) tube, shown in Figure 4, the bonding between the oxygen and the carbon atoms produces a new unoccupied band near the Fermi level, as displayed by the dotted line in Figure 4b, which is responsible for the reduction in the band gap. For the metallic or semimetallic SWNTs with $n = 3m$, the cycloaddition only introduces very small changes in the band gap, which is consistent with the experimental finding that only the semicon-

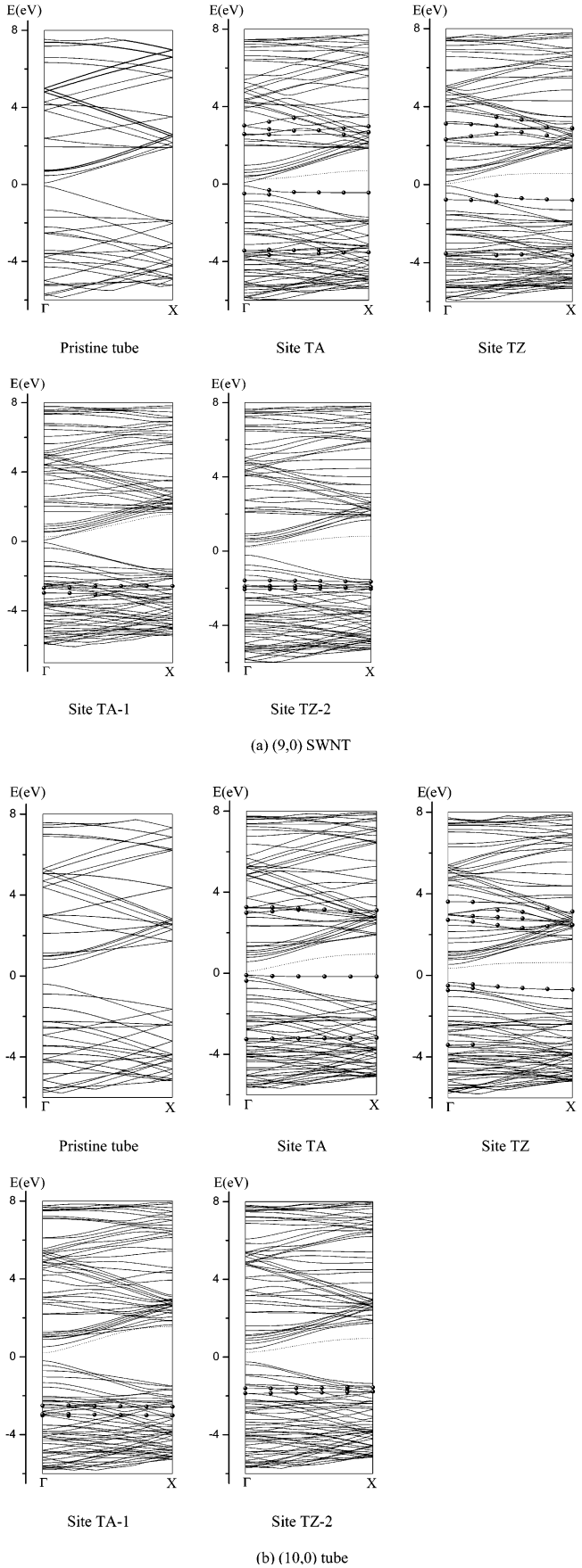

Figure 4. Calculated band structures for the pristine and oxygen chemisorbed carbon nanotubes, (a) (9,0) tube; and (b) (10,0) tube. The dots indicate the bands contributed by atomic orbitals on oxygen atoms, while the broken lines indicate the new conductive bands formed upon oxygen chemisorption.

ducting SWNTs exhibit electrical conductance change upon oxygen doping.[13]

For the epoxide structures, except $n = 6$, a trend of increase in the band gap is observed for the metallic tubes $n = 3m$. As shown in Figure 4a for the (9,0) tube, a new unoccupied band is also observed near the Fermi level in the band structures of a chemisorbed (9,0) tube. However, relative to the Fermi level, there is no significant decrease in the energies for this new band and the other conducting bands, while decreases in energy are observed for the occupied bands. The result is an increase in the band gap for the epoxide (9,0) tube. We have also calculated the DOSs for the pristine and chemisorbed tubes, but the changes near the Fermi level introduced upon chemisorption are small.

Conclusion

We have studied the chemisorption of singlet O_2 on a series of (n,0) zigzag SWNTs with $n = 6-15$, by first principles calculations. The process can be divided into two steps, a cycloaddition to a C−C bond, followed by the complete breaking of an O−O bond to form an epoxide structure.

For both the cycloaddition and epoxide structures, there is a general trend of decreases in the value of $-E_{ads}$ with increasing tube diameter. The reactivity is also dependent on the electronic structure, with the metallic tubes more reactive than the semiconducting tubes. Relative to a bare tube and a singlet oxygen, the cycloaddition step is exothermic only for (n,0) tubes with $n < 12$, while the step of epoxide formation is exothermic for all tubes studied (with $n \leq 15$). Our results indicate that for tubes with a diameter around 1 nm, it is possible to introduce two epoxy groups onto the tube wall by reactions with singlet O_2, which provide a possible route for chemical functionalization. On the other hand, the formation of an epoxy structure could also lead to the complete breaking of a C−C bond near the adsorption sites. The degradation of zigzag tubes by oxidation, upon exposure to air and sunlight, is likely a problem only for the tubes with a diameter less than 1 nm.

Such oxidation processes also lead to changes in the electronic structure. Generally, for the semiconducting tubes, the band gap is reduced for both the cycloaddition and epoxy products. For the metallic tubes, the cycloaddition step produces little change in the band gap, while an increase in the band gap is observed for the epoxy structure.

Acknowledgment. The reported works are supported by an Earmarked Grant (CUHK 4252/01P) from the Research Grants Council of the Hong Kong SAR Government. Y.F. Zhang also acknowledges supports from the National Science Foundation of China (20303002) and the funds from the Educational Commission of Fujian Provincial Government (K02012) and Fuzhou University. We are also grateful for the generous allocation of computer time on the clusters of PCs and AlphaStations at the Chemistry Department and the Center for Scientific Modeling and Computation, and on the high performance computing facilities at the Information Technology Service Center, all located at The Chinese University of Hong Kong.

References and Notes

(1) Iijima, S. *Nature* **1991**, *354*, 56.

(2) Sun, Y.; Fu, K.; Lin, Y.; Huang, W. *Acc. Chem. Res.* **2002**, *35*, 1096.

(3) Niyogi, S.; Hamon, M. A.; Hu, H.; Zhao, B.; Bhowmik, P.; Sen, R.; Itkis, M. E.; Haddon, R. C. *Acc. Chem. Res.* **2002**, *35*, 1105.

(4) Yim, W. L.; Gong, X. G.; Liu, Z. F. *J. Phys. Chem. B* **2003**, *107*, 9363.

(5) Hirsch, A. *Top. Curr. Chem.* **1998**, *199*, 1.
(6) Chiang, I. W.; Brinson, B. E.; Huang, A.; Willis, P. A.; Bronikowski, M. J.; Margrave, J. L.; Smalley, R. E.; Hauge, R. H. *J. Phys. Chem. B* **2001**, *105*, 8297.
(7) Zhou, W.; Ooi, Y.; Russo, R.; Papanek, P.; Luzzi, D. E.; Fischer, J. E.; Bronikowski, M. J.; Willis, P. A.; Smalley, R. E. *Chem. Phys. Lett.* **2001**, *350*, 6.
(8) Strano, M. S.; Dyke, C. A.; Usrey, M. L.; Barone, P. W.; Allen, M. J.; Shan, H.; Kittrell, C.; Hauge, R. H.; Tour, J. M.; Smalley, R. E. *Science* **2003**, *301*, 1519.
(9) Savage, T.; Bhattacharya, S.; Sadanadan, B.; Gaillard, J.; Tritt, T. M.; Sun, Y.-P.; Wu, Y.; Nayak, S.; Car, R.; Marzari, N.; Ajayan, P. M.; Rao, A. M. *J. Phys.: Condens. Matter*. **2003**, *15*, 5915.
(10) Collins, P. G.; Bradley, K.; Ishigami, M.; Zettl, A. *Science* **2000**, *287*, 1801.
(11) Bradley, K.; Jhi, S.-H.; Collins, P. G.; Hone, J.; Cohen, M. L.; Louie, S. G.; Zettl, A. *Phys. Rev. Lett.* **2000**, *85*, 4361.
(12) Tang, X.-P.; Kleinhammes, A.; Shimoda, H.; Fleming, L.; Bennoune, K. Y.; Sinha, S.; Bower, C.; Zhou, O.; Wu, Y. *Science* **2000**, *288*, 492.
(13) Chen, R. J.; Franklin, N. R.; Kong, J.; Cao, J.; Tombler, T. W.; Zhang, Y.; Dai, H. *Appl. Phys. Lett.* **2001**, *79*, 2258.
(14) Derycke, V.; Martel, R.; Appenzeller, J.; Avouris, Ph. *Appl. Phys. Lett.* **2002**, *80*, 2773.
(15) Heinze, S.; Tersoff, J.; Martel, R.; Derycke, V.; Appenzeller, J.; Avouris, Ph. *Phys. Rev. Lett.* **2002**, *89*, 106801.
(16) Lee, S. M.; Lee, Y. H.; Hwang, Y. G.; Hahn, J. R.; Kang, H. *Phys. Rev. Lett.* **1999**, *82*, 217.
(17) Mann, D. J.; Hase, W. L. *Phys. Chem. Chem. Phys.* **2001**, *3*, 4376.
(18) Sorescu, D. C.; Jordan, K. D.; Avouris, Ph. *J. Phys. Chem. B* **2001**, *105*, 11227.
(19) Ricca, A.; Bauschlicher, C. W., Jr.; Maiti, A. *Phys. Rev. B* **2003**, *68*, 035433.
(20) Chan, S. P.; Chen, G.; Gong, X. G.; Liu, Z. F. *Phys. Rev. Lett.* **2003**, *90*, 086403.
(21) Froudakis, G. E.; Schnell, M.; Muhlhauser, M.; Peyerimhoff, S. D.; Andriotis, A. N.; Menon, M.; Sheetz, R. M. *Phys. Rev. B* **2003**, *68*, 115435.
(22) Dresselhaus, M. S.; Dresselhaus, G.; Eklund, P. C. *Science of Fullerenes and Carbon Nanotubes*; Academic Press: San Diego, CA, 1996.
(23) Cohen, M. L. *Phys. Rev.* **1984**, *110*, 293.
(24) Payne M. C.; Teter M. P.; Allan D. C.; Arias T. A.; Joannopoulos J. D. *Rev. Mod. Phys.* **1992**, *64*, 1045.
(25) Kresse, G.; Furthmuller, J. *Phys. Rev. B* **1996**, *54*, 11169; *Comput. Mater. Sci.* **1996**, *6*, 15.
(26) Perdew, J. P. In *Electronic Structure of Solids'91*; Ziesche, P., Eschrig, H., Eds.; Academie Verlag: Berlin, 1991.
(27) Vanderbilt, D. *Phys. Rev. B* **1990**, *41*, 7892.
(28) Monkhorst, H. J.; Pack, J. D. *Phys. Rev. B* **1976**, *13*, 5188.
(29) Huber, K. P.; Herzberg, G. *Molecular Spectra and Molecular Structure: Constants of Diatomic Molecules*; Van Nostrand Reinhold: New York, 1979; Vol. 4.
(30) Saunders, V. R.; Dovesi, R.; Roetti, C.; Orlando, R.; Zicovich-Wilson, C. M.; Harrison, N. M.; Doll, K.; Civalleri, B.; Bush, I.; D'Arco, Ph.; Llunell M. *CRYSTAL2003 User's Manual*; University of Torino: Torino, 2003.
(31) Ricca, A.; Drocco, J. A. *Chem. Phys. Lett.* **2002**, *362*, 217.
(32) Yim, W. L.; Liu, Z. F. Submitted.
(33) Haddon, R. C. *Science* **1993**, *261*, 1545.
(34) Lu, X.; Tian, F.; Xu, X.; Wang, N.; Zhang, Q. *J. Am. Chem. Soc.* **2003**, *125*, 10459.
(35) Chen, Z.; Thiel, W.; Hirsch, A. *Chem. Phys. Chem.* **2003**, *1*, 93.
(36) Treacy, M. M. J.; Ebbesen, T. W.; Gibson, J. M. *Nature* **1996**, *381*, 678.
(37) Yakobson, B. I.; Brabec, C. J.; Bernholc, J. *Phys. Rev. Lett.* **1996**, *76*, 2511.
(38) Gao, G. H.; Cagin, T.; Goddard, W. A., III *Nanotechnology* **1998**, *9*, 184.
(39) Dag, S.; Gulseren, O.; Yildirim, T.; Ciraci, S. *Phys. Rev. B* **2003**, *67*, 165424.
(40) Dag, S.; Gulseren, O.; Ciraci, S. *Chem. Phys. Lett.* **2003**, *380*, 1.
(41) Walch, S. P. *Chem. Phys. Lett.* **2003**, *374*, 501.
(42) Kudin, K. N.; Bettinger, H. F.; Scuseria, G. E. *Phys. Rev. B* **2001**, *63*, 045413.
(43) Park, K. A.; Choi, Y. S.; Lee, Y. H.; Kim, C. *Phys. Rev. B* **2003**, *68*, 045429.
(44) Sun, G.; Kurti, J.; Kertesz, M.; Baughman, R. H. *J. Phys. Chem. B* **2003**, *107*, 6924.
(45) Barone, V.; Heyd, J.; Scuseria, G. E. *Chem. Phys. Lett.* **2004**, *389*, 289.